OCTOBER 01 2005

Vibroacoustics of three-dimensional drum silencer

Lixi Huang; Y. S. Choy

J. Acoust. Soc. Am. 118, 2313–2320 (2005)
https://doi.org/10.1121/1.2010353

Vibroacoustics of three-dimensional drum silencer

Lixi Huang[a] and Y. S. Choy
Department of Mechanical Engineering, The Hong Kong Polytechnic University, Kowloon, Hong Kong, China

(Received 6 December 2004; revised 11 June 2005; accepted 5 July 2005)

When a segment of a rigid duct wall is replaced by a membrane and is backed by a cavity, incident noise induces membrane vibrations and causes noise reflection. The reflection is effective over a broad band in the low-frequency region when a certain high tension is applied on the membrane in the axial direction of the duct. The device is thus called a drumlike silencer. The existing vibroacoustic theory is based on a two-dimensional duct model and the membrane is reduced to a one-dimensional string. This study extends the theory to three dimensions for the duct and two dimensions for the membrane which has all four edges fixed. It is shown, analytically, that the lateral tension is always detrimental to the silencing performance. However, the optimal performance of the one-dimensional string is recovered exactly when the lateral tension on the two-dimensional membrane vanishes despite the very different boundary conditions. The conclusion is validated experimentally, paving the way for the application of the drum silencer in which the cavity is completely separated from the gas flow in the duct.
[DOI: 10.1121/1.2010353]

PACS number(s): 43.50.Gf, 43.20.Tb, 43.20.Ks [DKW] Pages: 2313–2320

I. INTRODUCTION

The problem of duct noise is found in many industrial and domestic applications, such as ventilation systems and exhaust chimneys. Existing noise abatement techniques can be broadly categorized by three approaches: sound absorption, sound reflection, and active noise control using destructive acoustic interference. Lining a duct with sound absorbing material, mostly porous, has been very common and often the most reliable engineering solution (Mechel and Vér, 1992; Ingard, 1994). If, for chemical or other reasons within the exhaust gas, the use of a porous material is not desirable, alternative sound absorbing structures are used. Most such structures utilize the principle of Helmholtz resonator (Fuchs, 2001), of which microperforation is one (Maa, 1975, 1998). Like duct lining of fibrous material, arrays of Helmholtz resonators can also provide effective noise absorption for a broad frequency band. However, one of the drawbacks of sound absorption is that, in general, it does not work well for very low frequencies, such as those below 200 Hz. The reason is that air is essentially incompressible at low frequencies. A cavity housing the sound absorption material would appear to be small relative to the wavelength, and the rigid walls of the cavity constrain the motion of air which then appears to be stiff. The problem of air stiffness also occurs in the use of a loudspeaker as a secondary source in active noise control. The loudspeaker becomes very ineffective at low frequencies when its back is enclosed by a cavity with rigid walls. Without such a rigid cavity, a device of active noise control would cause noise leaking instead of noise cancellation.

In some cases, the technique of sound reflection is more convenient to apply, or is at least highly complementary to the use of sound absorption technique, the most typical example being the vehicle exhaust muffler. The principle behind this technique is the use of discontinuity of acoustic impedance in a duct, such as an expansion chamber. For the same degree of impedance discontinuity, a sound wave reflector could be equally effective for low and intermediate frequencies. However, to achieve a very high rate of noise reduction in the receiving end of the duct, the expansion chamber has to be very large. This contrasts with the technique of duct lining for which the principal requirement concerns its length in the direction of the duct axis. The sudden expansion creates serious problems for any flow the duct may carry. Flow separation may occur and it results in more noise. Besides, passband exists in an expansion chamber. These drawbacks have prompted the present authors to introduce a tensioned membrane as a means of achieving broadband sound reflection in the region of low frequencies. As shown in Fig. 1, the prototype device is, broadly speaking, an expansion chamber with two side-branch cavities covered by light membranes under a fairly high tension, hence the name drumlike silencer, or simply drum silencer, in our previous publications.

The development of the drum silencer up to this point is briefly summarized here. The starting point was the exploration of acoustic impedance discontinuity inspired by the property of flexible tube in human respiratory system (Huang *et al.*, 1995; Huang, 1999). The propagation of sound waves coupled with the flexual waves of a membrane tends to be much slower than the free sound waves in air. Such low wave speed has also been measured experimentally (Huang *et al.*, 2000). The crucial advantage of such flexible tube is the preservation of a smooth flow passage. When utilized as a silencer, this feature carries two benefits. The first is the absence of any extra air pressure loss, such as that caused by flow separation in an expansion chamber, and the associated

[a]Electronic mail: mmlhuang@polyu.edu.hk

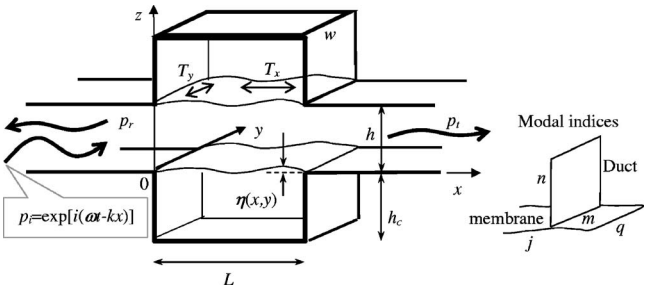

FIG. 1. Configuration of a drum silencer with two identical modules of cavity-backed membrane. Each cavity has a length of L, depth h_c, and width w.

extra noise from such turbulent flow. The second benefit is the complete separation of the gaseous flow in the duct from the cavity, which eliminates the chance of dust accumulation and other possible long-term environmental and maintenance problems. The complete separation of flow in the duct from the cavity also allows the use of a low impedance gas, such as helium, to fill the cavity to further enhance the silencer performance (Choy and Huang, 2003). Physically speaking, what happens in a drum silencer is as follows. When a sound wave is incident from the left-hand side of the device, it induces the membrane to vibrate and this vibration radiates sound in both left-hand and right-hand sides of the duct. The left-traveling waves form the reflected sound, while the right-traveling waves combine with the incident wave and form the transmitted sound. The principle of acoustic energy conservation guarantees that whatever amount of wave is reflected is accompanied by the same amount of reduction in the energy flux of the transmitted wave. In other words, the acoustic interference at the right-hand side is definitely destructive as the incident wave is the only energy flow source. Acoustically, the device behaves like a secondary source in the active noise control technique, the difference being the absence of sensors, actuators, and a control circuit. The important question of cavity air stiffness arises also, and the work has been carried out to optimize the design parameters such that the widest possible stopband is created with a given cavity volume (Huang, 2004). Both analytical (Huang, 2002) and experimental results (Choy and Huang, 2002) show that the performance of the drum silencer is very good.

It may be said that the use of membrane in noise abatement engineering is not entirely new. For example, panel absorbers were used in broadcasting studios and other architectural practices (Brown, 1964; Ford and McCormick, 1969; Sakagami *et al.*, 1996; Horoshenkov and Sakagami, 2001), membrane absorbers were also used as a splitter silencer in the form of arrays of Helmholtz resonators (Frommhold *et al.*, 1994). However, in all these applications, the membrane, or panel, is a component of resonator which works for a narrow frequency band, and the structural mass is a means to achieve a low resonance frequency. To the best of the authors' knowledge, the use of tensioned membrane to actively promote the vibroacoustic interaction for the purpose of wave reflection was new and unique (Huang, 1999).

The theoretical studies on the drumlike silencer have so far been confined to two dimensions for the duct, and one dimension for the membrane, which is essentially a string. However, the theoretical model was realistic enough to be simulated by an experimental rig to validate the theory (Choy and Huang, 2002). In such an experiment, the two edges of the membrane at $y=0$, w, where w is the membrane width, are free to move, and it in fact moves in step with the whole width of the membrane. With such a construction, the cavity is not air-tight, and it contradicts with the important potential environmental advantage of the device, namely the absolute separation between the duct and the cavity. To be air-tight, the four edges of the membrane have to be fixed on the duct walls so that the dusts from the gaseous flow are prevented from entering the cavity. Such boundary condition would inevitably make the membrane response highly two-dimensional, and the sound waves in the duct and cavity three-dimensional. The main motivation behind the current study is the concern of whether a membrane fixed on all edges would still yield the same silencing performance as the rather idealistic two-dimensional (2D) model. This concern arises since the constraints at all edges apparently reduce the response of the membrane to incident sound.

In what follows in Sec. II, complete formulation is given for the solution of the three-dimensional (3D) problem with all membrane edges fixed. The effect of the lateral tension, T_y, is studied in detail, and is found to be detrimental to the silencing performance. The special design of $T_y=0$ is studied in Sec. III. It is shown, analytically, that a 3D device with such property gives identical silencing performance as a drum silencer constructed on the basis of the 2D model despite the very different boundary conditions. This conclusion is encouraging and is validated experimentally.

II. THEORY

In the following, the formulation for calculating the response of the two-dimensional membranes in a three-dimensional duct is presented following the standard Galerkin procedure. The resulting set of linear equations is solved by general matrix inversion techniques. The effect of modal truncation is discussed first, followed by the study of the effect of the lateral tension, T_y.

A. The three-dimensional model

As shown in Fig. 1, a rectangular duct of height h and width w is equipped with two rigid-walled cavities of length L and depth h_c on two opposite sides. Each cavity is covered by a membrane of length L and width w, which forms part of the otherwise rigid duct wall. The membranes are fixed at the leading and trailing edges of $x=0$, L, as well as at the other two edges at $y=0$, w, which are henceforth called the lateral edges. A tensile force of T_x is applied on the membrane in the axial direction of the duct, and another tensile force of T_y is applied in the y direction. Plane incident wave p_i is introduced from the left-hand side with a unit amplitude. This wave induces membrane response of displacement $\eta(x,y,t)$ in the z direction with velocity $V=\partial\eta/\partial t$. The vibration radiates sound and imposes a radiation pressure on the membrane surface. The problems of acoustics and membrane vibration are fully coupled. As shown in the figure, the final reflected wave is denoted as p_r, and the transmitted wave p_t

assuming no further reflection in the far right-hand side. The transmission loss TL is defined as follows for harmonic incident wave p_i:

$$p_i(x,t) = \exp[i(\omega t - kx)],$$
$$\mathrm{TL} = 20\log_{10}|p_i/p_t| = -20\log_{10}|p_t|, \tag{1}$$

where $\omega = 2\pi f$ and $k = \omega/c_0$ are the angular frequency and the wave number, respectively, f is the frequency, and c_0 is the speed of sound in free space. The task now is to choose a set of properties for the membrane and cavity which would yield a TL higher than a certain criterion value over a widest possible continuous frequency band $f \in [f_1, f_2]$. The ratio f_2/f_1 can be seen as a logarithmic bandwidth, which is adopted as the quantity to be maximized in an optimization exercise for which more details are given in Huang (2004). Briefly, f_2/f_1 is maximized for a given cavity volume Lh_c and the main variables are the membrane tension and cavity shape. The motivation behind using such a bandwidth definition is the desire to put due emphasis on the low-frequency performance, which is a technical challenge in duct noise abatement.

The dynamics equation for the lower membrane with its nominal position at $z=0$ is

$$m_s\frac{\partial^2\eta}{\partial t^2} - T_x\frac{\partial^2\eta}{\partial x^2} - T_y\frac{\partial^2\eta}{\partial y^2} + (p_i + \Delta p) = 0, \tag{2}$$

where m_s is the mass per unit area of the membrane, $\Delta p = p_+ - p_-$ is the fluid loading acting on the upper (+) and lower (−) sides of the membrane induced by the membrane vibration itself. The solution for the problem with two identical membranes is simplified to a problem in which one membrane is installed in a duct of height $h/2$ and the symmetric plane of $z=h/2$ is replaced by a solid wall. With this simplification, the presence and the effect of the upper membrane at $z=h$ are ignored in the subsequent theoretical development. However, the duct height h is still used in the formulation as a length scale.

Notice that the effect of the bending stiffness, $B\partial^4\eta/\partial x^4$, has been left out of the dynamics equation (2). Here, $B = Es^3w/12$ is the flexual rigidity of the membrane of thickness s, width w, and E is the Young's modulus. The ratio of the neglected bending term, $B\partial^4\eta/\partial x^4$, to that of the tensile force, $T_x\partial^2\eta/\partial x^2$, is examined here for the second *in vacuo* vibration mode, $\eta = \sin(2\pi x/L)$, which is shown later to be the most important mode. The ratio is

$$\left|\frac{B\partial^4\eta/\partial x^4}{T_x\partial^2\eta/\partial x^2}\right| = \frac{Es^3w(2\pi)^2}{12T_xL^2}. \tag{3}$$

For the typical configuration used in the experiment of the current study, a stainless steel of thickness $s=0.025$ mm is used, $E=190$ GPa, $w=0.1$ m, $L=0.5$ m, and $T_x=750$ N. The ratio turns out to be $5.21\times10^{-6} \ll 1$, confirming that the structure is truly a membrane instead of a plate.

B. Solution to the model problem

The Galerkin procedure to solve the coupled problem is outlined as follows. First, the fluid loading Δp is divided into three parts:

$$\Delta p = p_{+\mathrm{rad}} - (p_{-\mathrm{rad}} + p_{-\mathrm{ref}}), \tag{4}$$

where $p_{+\mathrm{rad}}$ and $p_{-\mathrm{rad}}$ are the radiation sound pressures on the upper and lower membrane surfaces at $z=0+$ and $0-$, respectively, when the two vertical cavity walls at $x=0$ and L are temporarily ignored. $p_{-\mathrm{ref}}$ is the sound reflected by the two vertical cavity walls. One way to relate these pressures with the vibration velocity V is to express the coupled membrane response as a combination of *in vacuo* membrane vibration modes. For membranes fixed on all four edges, the *in vacuo* modes, denoted by φ, are simply sine functions, as shown in the following,

$$V(x,y,t) = \frac{\partial\eta}{\partial t} = e^{i\omega t}\sum_{j=1}^{\infty}\sum_{q=1}^{\infty} V_{jq}\varphi_{jq}(x,y),$$
$$V_{jq} = \frac{4}{Lw}\int_0^w\left[\int_0^L V\varphi_{jq}dx\right]dy, \tag{5}$$
$$\varphi_{jq}(x,y) = \sin(j\pi x/L)\sin(q\pi y/w),$$

where j and q are modal indices in x and y directions, respectively, and the double summations are abbreviated as Σ_{jq} henceforth. For convenience, modal indices for the duct acoustics and membrane vibration are indicated at the right-hand side of Fig. 1.

The crucial step now is to relate the modal amplitudes V_{jq} to the induced fluid loading Δp. To do so, sound radiation is first considered for a prescribed modal vibration of a unit amplitude, $V_{jq}=1$, and the resultant fluid loading, denoted as $e^{i\omega t}\Delta p^{(jq)}(x,y)$, is also expanded into *in vacuo* modes of indices $j'q'$,

$$Z_{jqj'q'} = \frac{4}{Lw}\int_0^w\left[\int_0^L \Delta p^{(jq)}\varphi_{j'q'}dx\right]dy,$$
$$\Delta p = e^{i\omega t}\sum_{j,q} V_{jq}\sum_{j',q'} Z_{jqj'q'}\varphi_{j'q'}. \tag{6}$$

Here, the matrix of $Z_{jqj'q'}$ can be called the modal impedance of the membrane. When Eq. (2) is multiplied by φ_{jq} and integrated over the membrane surface, it becomes a set of linear equations,

$$\mathcal{L}_{jq}V_{jq} + \sum_{j,q,j',q'} Z_{jqj'q'}V_{jq} + I_{jq} = 0,$$
$$j = 1,2,3,\ldots, \quad q = 1,2,3,\ldots, \tag{7}$$

where $\mathcal{L}_{jq}$ is the structural operator and I_{jq} is the modal amplitude of the incident wave p_i, as shown below:

$$\mathcal{L}_{jq} = m_s i\omega + \frac{T_x}{i\omega}\left(\frac{j\pi}{L}\right)^2 + \frac{T_y}{i\omega}\left(\frac{q\pi}{w}\right)^2,$$

$$I_{jq} = \underbrace{\frac{2}{w}\int_0^w \sin\left(\frac{q\pi y}{w}\right)dy}_{F_q} \times \underbrace{\frac{2}{L}\int_0^L p_i \sin\left(\frac{j\pi x}{L}\right)dx}_{I_j^{(2D)}},$$

$$F_q = 2\frac{1-\cos(q\pi)}{q\pi} = \begin{cases} \frac{4}{q\pi}, & \text{odd } q \\ 0, & \text{even } q \end{cases},$$

$$I_j^{(2D)} = 2j\pi e^{ikL/2}\left[\frac{1-e^{i(-kL+j\pi)}}{(j\pi)^2-(kL)^2}\right]. \tag{8}$$

The key to solving Eq. (7) is finding the modal impedance $Z_{jqj'q'}$. To do so, $p_{+\text{rad}}, p_{-\text{rad}}$, and $p_{-\text{ref}}$ are needed. Formulations for $p_{+\text{rad}}$ and $p_{-\text{rad}}$ are available in literature, such as Doak (1973), and $p_{-\text{ref}}$ is given in Huang (2002). Since all three pressure components have essentially the same functional relationships in the directions of y and z, only $p_{+\text{rad}}$ is shown below for essential discussions. Dropping the common time dependence factor e^{iwt} from this point onwards, the complex amplitude of the radiation pressure is written as

$$\begin{aligned} p_{+\text{rad}}(x,y,z) &= \frac{\rho_0}{2A}\sum_{m=0}^{\infty}\sum_{n=0}^{\infty} c_{mn}\psi_{mn}(y,z) \\ &\quad \times \int_0^w \left[\int_0^L \psi_{mn}(y',z')V(x',y')G_{mn}(x,x')dx'\right] \\ &\quad \times dy', \end{aligned} \tag{9}$$

$$\begin{aligned} G_{mn}(x,x') &= H(x-x')e^{-ik_{mn}(x-x')} + H(x'-x)e^{+ik_{mn}(x-x')} \\ &= \cos[k_{mn}(x-x')] - i\,\sin[k_{mn}|x-x'|], \end{aligned}$$

where primes indicate the source coordinates on the membrane at $z'=0$, ρ_0 is the density of the undisturbed fluid, $G_{mn}(x,x')$ plays the role of a Green function, which contains Heaviside functions H, ψ_{mn} is the duct acoustics modal function, c_{mn} and k_{mn} are, respectively, the associated modal wave speed and wave number, which are defined in the following. The duct acoustics modes, denoted by ψ_{mn}, satisfying the rigid wall condition and the homogeneous wave equation in air,

$$\left(\frac{\partial^2}{c_0^2\,\partial t^2} - \nabla^2\right)p = 0, \quad \nabla p_{\text{wall}} = 0, \tag{10}$$

are

$$p = \psi_{mn}(y,z)\exp[i(\omega t \pm k_{mn}x)], \quad m,n = 0,1,2,3,\ldots,$$

$$k_{mn} = \frac{\omega}{c_{mn}}, \quad c_{mn} = \frac{ic_0}{\sqrt{(m\pi/kw)^2 + (n\pi/kh)^2 - 1}},$$

$$\psi_{mn} = \sqrt{(2-\delta_{0m})(2-\delta_{0n})}\cos\left(\frac{m\pi y}{w}\right)\cos\left(\frac{n\pi z}{h}\right),$$

$$\frac{1}{A}\int\int_A \psi_{mn}\psi^*_{m'n'}dA = \begin{cases} 0, & (m,n) \neq (m',n') \\ 1, & (m,n) = (m',n'), \end{cases} \tag{11}$$

where $A = h \times w$ is the cross section of the duct, and asterisk in the last expression indicates the complex conjugate. Note that the modal index for the common edge direction of y is q for the membrane vibration but m is used for the duct acoustics. The radiation loading on the membrane at $z=0$ caused by the membrane vibration of mode (j,q) with a unit amplitude is denoted as $p_{+\text{rad}}^{(jq)}$,

$$\begin{aligned} p_{+\text{rad}}^{(jq)} &= \frac{\rho_0}{2A}\sum_{m=0}^{\infty}\sum_{n=0}^{\infty} c_{mn}(2-\delta_{0m})(2-\delta_{0n})\cos\left(\frac{m\pi y}{w}\right) \\ &\quad \times \int_0^w \cos\left(\frac{m\pi y'}{w}\right)\sin\left(\frac{q\pi y'}{w}\right)dy' \\ &\quad \times \int_0^L \sin\left(\frac{j\pi x'}{L}\right)G_{mn}(x,x')dx', \end{aligned} \tag{12}$$

and the modal impedance from this term is denoted as $Z_{jqj'q'}^{(+\text{rad})}$,

$$Z_{jqj'q'}^{(+\text{rad})} = \frac{2\rho_0 L}{h}\mathcal{I}_{jj'}\sum_{m=0}^{\infty}\sum_{n=0}^{\infty}(2-\delta_{0m})(2-\delta_{0n})c_{mn}C_{mq}C_{mq'},$$

$$\begin{aligned} C_{mq} &= \int_0^1 \cos(m\pi\xi)\sin(q\pi\xi)d\xi \\ &= \begin{cases} \frac{2q/\pi}{q^2-m^2}, & m+q = \text{odd} \\ 0, & m+q = \text{even}, \end{cases} \end{aligned} \tag{13}$$

$$\begin{aligned} \mathcal{I}_{jj'} &= \frac{1}{L^2}\int_0^L \sin(j'\pi x/L) \\ &\quad \times \left[\int_0^L \sin(j\pi x'/L)G_{mn}(x,x')dx'\right]dx \\ &= \frac{jj'\pi(e^{ij\pi} - e^{-ik_mL})(e^{ij\pi} + e^{ij'\pi})}{[(k_mL)^2 - (j\pi)^2][(k_mL)^2 - (j'\pi)^2]} \\ &\quad - \frac{ik_mL\delta_{jj'}}{(k_mL)^2 - (j\pi)^2}. \end{aligned}$$

The double axial integration $\mathcal{I}_{jj'}$, is unlikely to vanish for any mode due to the different nature of the traveling acoustic waves and the standing waves on the structure. However, subtle modal coupling arises from $C_{mq}C_{mq'}$. For example, odd vibration mode of $q=1$ radiates sound which propagates as even duct acoustics modes of $m=0,2,4,\ldots$, and these acoustics modes in turn add loading on odd membrane modes of $q'=1,3,5,\ldots$. The conclusion is that odd membrane vibration modes put loading on odd modes and not on even modes, vice versa. Obviously, self loading for $q'=q$ is the strongest.

There is a complete decoupling between odd and even modes in the y direction. The set of linear equations in Eq. (7) can be separated into two sets and solved separately. The subset of equations for the even m modes are homogeneous since the incident wave p_i does not add load on even m

modes, as can be seen from the y-integration for F_q and I_{jq} in Eq. (8). This means that all even q modes, $q=2,4,6,\ldots$, should vanish if the determinant for the set of equations for the even modes does not vanish. When the determinant does vanish, the system experiences free vibration without excitation. As can be seen in the following, such a free vibration does not radiate sound into the far field, and the system therefore does not have fluid damping. A completely lossless system could have a real eigenfrequency for these even modes in the low-frequency range. In reality, there is always some damping present in the system. It is therefore argued that these even modes are not excited at all. Note that there is also a complete decoupling of modal impedance between odd and even modes in the axial direction, as shown earlier in Huang (2002). But the plane incident wave p_i has loading on both odd and even axial modes j. Therefore, both odd and even axial modes are excited.

Substituting the modal coefficient I_{jq} given in Eq. (8) and the modal impedance given in Eq. (13) into the linear equations of Eq. (7), the task of solution becomes essentially the inversion of matrix. Once the membrane response is found, the far field sound radiation can be calculated from Eq. (9) considering only the plane wave mode, $m=n=0$ for frequencies below the cut-on frequency of the duct, $\omega < \pi/h, \pi/w$. The combination of the downstream radiation wave with the incident wave forms the transmitted wave, while the upstream radiation becomes the reflection wave. The reflected wave is

$$p_r = p_{+\mathrm{rad}x\to-\infty} = \frac{\rho_0 c_0}{2A} e^{ikx} \int_0^L V_w(x') e^{-ikx'} dx',$$

$$V_w(x) = \frac{1}{w}\int_0^w V(x,y)dy = \sum_{j=1}^{\infty} V_j \varphi_j(x), \tag{14}$$

$$V_j = \frac{2}{L}\int_0^L V_w(x)\varphi_j(x)dx, \quad \varphi_j(x) = \sin\left(\frac{j\pi x}{L}\right),$$

where the membrane vibration velocity V is simply averaged over the width w and denoted as V_w, and the modal index q is dropped when $V_w(x)$ is expanded in the axial direction. The integration for Eq. (14) is identical to that of the 2D silencer (Huang, 2002). In fact, it is shown in the next section that the reflected wave for a 3D silencer with $T_y=0$ is identical to that of a 2D silencer.

C. Modal truncation and 2D membrane response

In actual calculations, the number of modes has to be truncated for Eq. (7), and the solution should be scrutinized carefully before being accepted. Denote the axial number of modes as N_j and the lateral number of modes as N_q, the convergence of solution as these numbers increase is shown in Fig. 2(a). In this study, $N_q=2N$ is specified as it is found that more lateral modes are needed when the lateral tension T_y is low. The following set of geometry and membrane properties are chosen as the testing case, for which the 2D analytical results were obtained earlier (Huang, 2002):

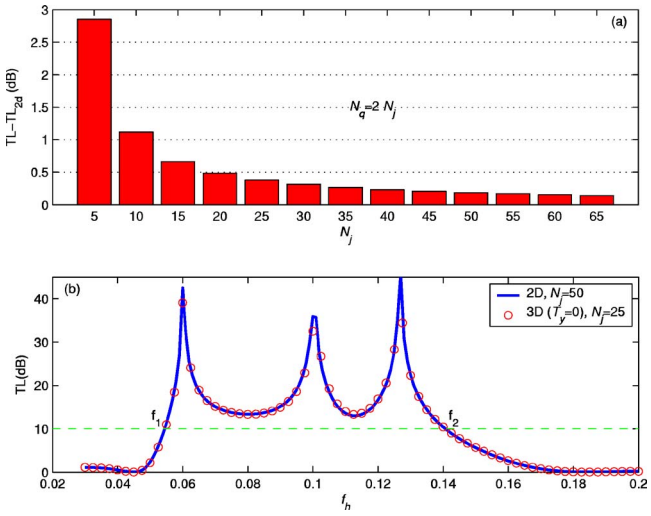

FIG. 2. (Color online) Convergence test for the modal truncation by comparison with the solution for the 2D silencer. (a) The error transmission loss for $f_h=0.11$ decreases with the mode number used, and (b) the close agreement between the transmission loss spectrum calculated by $N_j=25$.

$$L=5h, \quad h_c=w=h, \quad T_x=0.475(\rho_0 c_0^2 h^2),$$
$$T_y=0, \quad m_s/(\rho_0 h)=1 \tag{15}$$

For convenience, dimensionless frequency f_h and tensile forces, T_{xh}, T_{yh}, are defined as follows:

$$f_h=\frac{fh}{c_0}, \quad T_{xh}=\frac{T_x}{\rho_0 c_0^2 h^2}, \quad T_{yh}=\frac{T_y}{\rho_0 c_0^2 h^2}. \tag{16}$$

Tests are first conducted to see whether and how the results approach the 2D theory of Huang (2002) when N_j is gradually increased. When N_j is small, the main region of deviation between the 2D and 3D theories is found between the second and third peaks in the TL spectra. The dimensionless frequency of $f_h=0.11$ is therefore chosen as the test frequency to examine the effect of N_j on the results. At this frequency, TL=13.58 dB is predicted by the 2D theory with $N_j=50$, and the deviation by the 3D results is shown in Fig. 2(a). It is found that, beyond a certain moderate N_j, e.g., 25, the solution improvement becomes marginal. So, $N_j=25$ is chosen for the calculation of the 3D silencer for the whole frequency range. The result is compared with the 2D spectrum in Fig. 2(b) where the 3D result is shown in open circles and the 2D results in solid line. When a criterion value of 10 dB is used, the stopband in the figure is between $f_1=0.0545$ and $f_2=0.1406$, with a ratio of $f_2/f_1=2.58$.

Typical membrane responses for the frequency of $f_h=0.11$ are shown in Fig. 3. The top row is for $T_{yh}=0$, while the bottom row for $T_{yh}=0.02$, both with axial tension $T_{xh}=0.475$. The instantaneous vibration velocity distribution is shown in Figs. 3(a) and 3(c). As shown in Fig. 3(a), the membrane without lateral tension essentially behaves like a one-dimensional (1D) string in the sense that the membrane displacement rises very sharply from the fixed lateral edges, $y=0$, w, to the almost constant value over the central region.

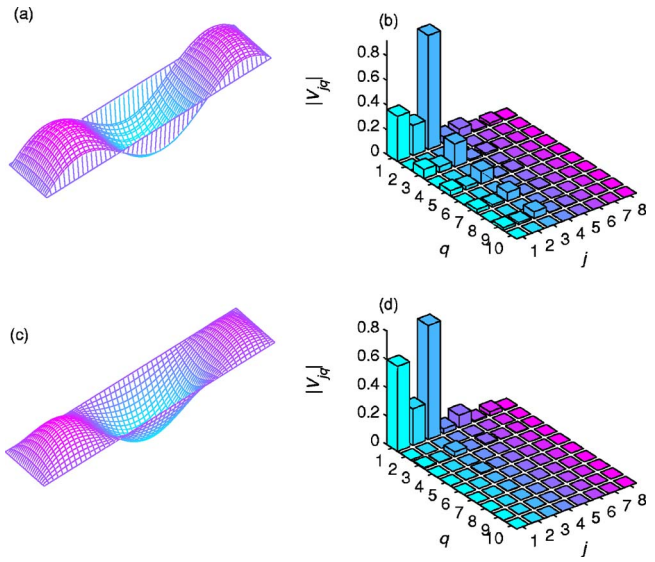

FIG. 3. (Color online) Comparison of membrane response for lateral tension $T_y=0$, for (a) and (b), and $T_y=0.02$, for (c) and (d). (a) and (c) The instantaneous membrane vibration velocity. (b) and (d) The distribution of the modal amplitudes.

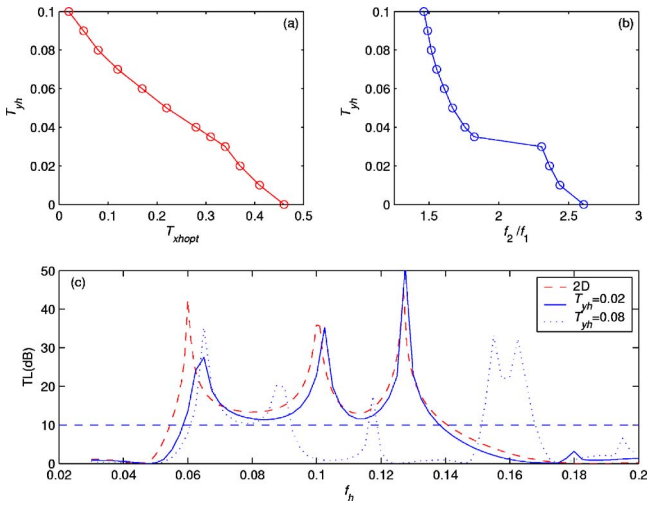

FIG. 4. (Color online) Variation with transverse tension T_{yh}. (a) The decrease of the optimal axial tension $T_{xh\text{opt}}$ as T_{yh} increases. (b) The reduction of the bandwidth of the optimal design using 10 dB as the criterion of stopband. (c) Comparison of the optimal transmission loss spectrum for the 2D configuration with the 3D configuration with $T_{yh}=0.02$, 0.08.

On the contrary, Fig. 3(c) shows that a rather smooth and fully two-dimensional distribution is found for the membrane with a small lateral tension.

The modulus of the membrane modal coefficient, $|V_{jq}|$, are shown in Figs. 3(b) and 3(d) as bar charts. Note that the modes with even q are absent since only odd q can be excited by a plane wave. For the odd modes, the decay with q is also reasonably fast. The largest responses in both cases are located near the first three axial modes. Comparing the two subfigures, it is found that a small T_{yh} can alter the membrane response drastically.

D. Effect of transverse tension

When a residual transverse tension T_{yh} is present, the system becomes truly three dimensional. It is found that the optimal design parameters are affected by T_{yh}. Following the procedure of Huang (2004) with a threshold transmission loss value of 10 dB, and using the parameters listed in Eq. (15), the optimal axial tensile forces $T_{xh\text{opt}}$ and the stopband parameters f_1, f_2 are found. The results are shown in Fig. 4 as a function of T_{yh}, the latter being shown as the vertical coordinate. Figure 4(a) shows that $T_{xh\text{opt}}$ diminishes rapidly as T_{yh} increases. A rather sudden change occurs near $T_{yh}=0.03$. This is partly due to the fact that the cavity is slender, so that any tension across the duct width causes a lot of stiffness effect. Figure 4(b) shows that, as T_{yh} increases, the stopband ratio f_2/f_1 also shrinks very rapidly. The optimal spectra under two typical $T_{yh}>0$ conditions are shown in Fig. 4(c). A small $T_{yh}=0.02$ is seen to make the stopband narrower with a higher starting frequency for the band, f_1, and a lower end frequency f_2. The frequency gap between the second and third peaks is also narrowed. Further increase in T_{yh} to 0.08 causes the merge of the second and third peaks, leading to a rather narrow, two-peak stopband. Similar peak movement can also be observed when the axial tensile force T_{xh} is increased beyond the optimal level when T_{yh} is absent. In conclusion, the effect of T_{yh} is generally considered to be counterproductive.

III. MEMBRANE WITHOUT LATERAL TENSION

In the following it is shown analytically that, when $T_y=0$, a two-dimensional membrane fixed on all edges performs exactly the same as a membrane with free edges behaving like a 1D string. Since this performance is also found to be the best in the last section, an experimental validation is given.

A. Plane wave solution

Equation (14) shows that the width-averaged membrane vibration velocity $V_w(x)$ alone determines the far field reflection, hence the silencing performance. In order to find V_w, Eq. (2) can be integrated over y. Assuming that the membrane surface density m_s and the axial tensile force T_x are not functions of y, the y integrations of the first two terms of Eq. (2) produce no functional changes except that the 2D displacement $\eta(x,y,t)$ is replaced by its 1D counterpart, say $\eta_w(x,t)=w^{-1}\int_0^w \eta(x,y,t)dy$. The same is true for the incident wave p_i which is also not a function of y. The question now is whether the same holds for the vibration induced fluid loading Δp, for which the upper surface term $p_{+\text{rad}}$ is given in Eq. (9).

When the modal function $\psi_{mn}(x,y)$ in Eq. (9), which contains $\cos(m\pi y/w)$, is integrated over y, the only contribution comes from the modes with $m=0$ while n can be any integer. These modes can be called two-dimensional duct acoustics modes with index m dropped,

$$\psi_n(z) \equiv \psi_{0n} = \sqrt{2-\delta_{0n}}\cos(n\pi z/h), \quad c_n \equiv c_{0n}. \tag{17}$$

Finally, the width-averaged loading from Eq. (9) becomes

$$\bar{p}_{+\mathrm{rad}}(x) = \frac{\rho_0}{2A}\sum_{n=0}^{\infty} c_n(2-\delta_{0n})\int_0^L G_{mn}(x,x')V_w(x')dx'. \tag{18}$$

It can be shown that similar results hold for the lower surface radiation pressure $p_{-\mathrm{rad}}$ and the cavity wall reflection pressure $p_{-\mathrm{ref}}$. The consequence of these results is that Eq. (2) can be formulated in a closed-form for the y-averaged membrane vibration velocity $V_w(x)$ using its expansion into the string vibration modes φ_j with modal coefficients V_j, as shown in the following:

$$\begin{aligned}
&\mathcal{L}_j V_j + \sum_{j,j'} Z_{jj'}V_j + I_j = T_y U_j, \quad j=1,2,3,\\
&\mathcal{L}_j = m_s i\omega + \frac{T_x}{i\omega}\left(\frac{j\pi}{L}\right)^2, \quad I_j = \frac{2}{L}\int_0^L p_i\varphi_j dx,\\
&U_j = \frac{2}{L}\int_0^L \left[\frac{\partial\eta}{\partial y}\right]_0^w \varphi_j(x)dx,\\
&Z_{jj'} = \frac{2}{L}\int_0^L \overline{\Delta p_j}(x)\sin(j'\pi x/L)dx,
\end{aligned} \tag{19}$$

where U_j is a stiffness term arising from the fixed lateral edges, and the width-averaged loading $\overline{\Delta p_j}$ depends only on V_w or V_j. When $T_y=0$, the term with the unknown U_j disappears, and the whole three-dimensional problem is reduced to two dimensions in which the membrane vibration is represented by the width-averaged velocity $V_w(x)$, and the modal impedance $Z_{jj'}$ is calculated purely on the basis of V_w with a total disregard for the boundary conditions at $y=0, w$. Since $Z_{jj'}$ does not contain any contribution from modes of $m>0$, and the excitation term I_j is identical to that in the 2D model, it follows that V_w is identical to the string displacement in the 2D model. The restriction of $\eta=0$ at the two edges of $y=0, w$ means that the induced vibration elsewhere is increased to compensate for the lateral edge constraints. In terms of the actual acoustic field around the membrane of finite width w, the structural boundary conditions at $y=0, w$ do influence the outcome. Higher order modes of $m>0$ exist but do not propagate. They become a purely reactive near-field oscillation which does not even influence the virtual mass on the width-averaged membrane response.

In fact, the above-presented analysis can be shown to hold when the membrane is not a rectangular piece of width w, but of any shape lined over a duct of any cross section, such as a circular duct with or without a solid clamp over the perimeter of the curved membrane. In the case of a circular duct, y in the above-presented analysis is replaced by the circumferential coordinate s and z is changed to radius r. Details of the modal functions ψ_{jq} and φ_{mn} would be quite different, but the method of plane wave solution using perimeter-integration stands. When $T_y>0$, or when m_s, T_x are functions of y, the full three-dimensional (3D) solution for the duct acoustics and the 2D solution for the membrane vibration have to be sought.

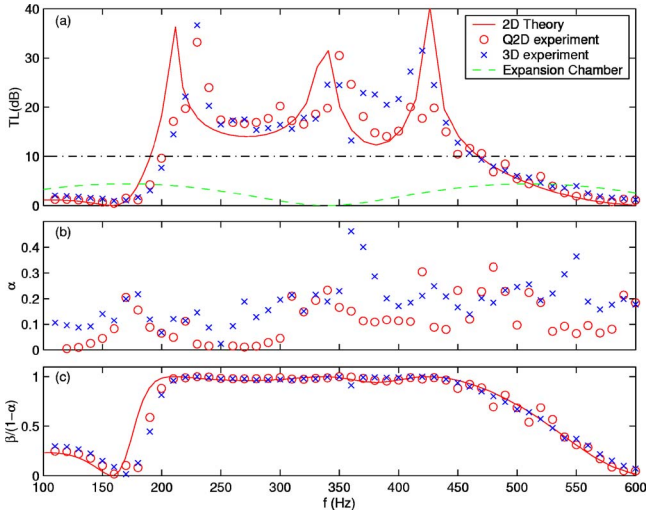

FIG. 5. (Color online) Comparison of the experimental data for the Q2D design (○) nd the 3D design (×) with the 2D theoretical prediction (solid line). (a) The transmission loss, (b) the sound energy absorption coefficient, and (c) the relative sound energy reflection coefficient.

B. Experimental validation

In order to validate the main conclusion that the membrane with all four edges fixed should perform the same way as one with two free lateral edges at $y=0, w$, experiments were conducted. The former configuration is called the 3D design, while the latter is called quasi-two-dimensional design denoted as Q2D. The procedure and methodology of the experiment are identical to that described in Choy and Huang (2002) where the Q2D design was used. Briefly, the standing wave pattern in the rectangular duct was resolved by the two-microphone method, while the transmission loss was deduced by the two-load method. The duct used had a dimension of $h=10$ cm by $w=10$ cm cross section, and the membrane had a length of $L=5h=0.5$ m and depth $h_c=h=10$ cm. The membrane was made of stainless steel, and the ratio of membrane to air mass calculated by $m_s/(\rho_0 h)$ was 1.4. The optimal tensile force predicted was close to $T_x=0.53(\rho_0 c_0^2 h^2)=750$ N. An optimal design here refers to the set of parameters with which the drum silencer attains the broadest continuous stopband of TL$\geqslant$10 dB. Note that the bandwidth is calculated as the ratio of the upper to lower frequency limits of the stopband (Huang, 2004). In Fig. 5, the experimental data from the Q2D design (○) and the 3D design (×) are plotted with the theoretical prediction (solid line) for the true 2D model (Huang, 2002). The dashed line is the 1D theory of the performance of an expansion chamber formed by the two cavities used in the drum silencer, and it is shown to be much lower in the stopband offered by the two drum silencers. Figure 5(a) compares TL, Fig. 5(b) shows the sound energy absorption coefficient, $\alpha=1-(|p_r|^2+|p_t|^2)$, measured in the experiment, Fig. 5(c) compares the relative sound energy reflection coefficient which is defined in the following. Several observations and discussions are given as follows.

(1) Figure 5(b) shows that a certain significant amount of sound energy absorption occurs in the experiment (between 10% and 20%), but the absorption is assumed to

be zero in theory. This discrepancy is not surprising. It is very hard to model energy dissipation mechanisms that occur in experiment with much theoretical certainty (Choy and Huang, 2002). Factors which may contribute to such energy dissipation include viscous friction between the air and the duct wall, possible duct wall vibration at low frequencies, sound leaking at some connection joints, material friction within the membrane and especially around membrane edges. Since the purpose of the drum silencer is for wave reflection, such additional damping is not pursued further theoretically. Besides, the damping may not be entirely beneficial in terms of TL as excessive damping has been shown to stifle the membrane vibration and wave reflection (Huang, 2004).

(2) As shown in Figs. 5(a) and 5(c), there is a frequency shift between the experimental data and the theoretical prediction around all three theoretical peaks of TL spectrum. This could be a result of measurement error for the tensile stress as it is difficult to fix the strain gauge on the thin and slippery membrane. The actual tensile force could be higher than 750 N. The disparity between theory and experiment, especially for the 3D design, is most significant between the second and third spectral peaks. There are two possibilities for this. First, the membrane had some residual tension in y direction when effort was made to flatten it. It is not uncommon that the membrane is a little crinkled during the experiment since the two clamps at $x=0$, L do not have very uniform gripping on the slippery membrane. In fact, the residual tension could be present in both Q2D and 3D experiments. In the case of the 3D experiment, a residual tension would lead to cross coupling between odd and even modes. If the membrane is crinkled, vibrations of complex modes would also lead to excessive damping of the system energy.

(3) Having considered the possible mechanisms of energy damping, a relative reflection coefficient, $\beta/(1-\alpha)$, where $\beta=|p_r|^2$, is introduced to examine to what extent the drum silencer reflects waves which are not absorbed, $1-\alpha$. The relative reflection is plotted in Fig. 5(c). Comparing Fig. 5(c) with Fig. 5(a), it is found that the collapse of experimental data on the theoretical prediction (solid line) for $\beta/(1-\alpha)$ is much better than that of TL or β (not shown).

(4) Notwithstanding all the differences between theory and experimental data, Figs. 5(a) and 5(c) show that there is a general agreement between the Q2D and the 3D experimental results throughout the whole stopband from about 200 to 450 Hz if 10 dB is used as a criterion value for the stopband. There is also a general agreement between the experimental data and the theoretical prediction.

IV. CONCLUSIONS

A theoretical study has been carried out to reveal the equivalence of the performance of a drum silencer with all membrane edges fixed and that simulating a two-dimensional model, the tension in the cross-sectional direction being zero. This result is brought out analytically and validated by experiment. The validation provides assurances that the cavity can be truly air-tight so that potential environmental advantages of the drum silencer can be realized. The reason why they are equivalent is that only the width-averaged membrane response is relevant to wave reflection into the far field, and the width-averaged response is decoupled from transverse modes. The latter only exists as a near field supplement to the problem of acoustic scattering by tensioned membranes. The conclusion actually holds for ducts with any cross sections.

The effect of transverse tension is found to be counterproductive as far as the performance of the drum silencer is concerned. In a real experiment, some residual transverse tension may always exist, but its negative impact would be small since the system does not behave singularly when the transverse tension changes.

ACKNOWLEDGMENT

The research carried out in this study was supported by grants from the Research Grants Committee of the Hong Kong SAR Government (PolyU 5169/02E, PolyU5298/03E).

Brown, S. (**1964**). "Acoustic design of broadcasting studios," J. Sound Vib. **1**, 239–257.

Choy, Y. S., and Huang, L. (**2002**). "Experimental studies of a drumlike silencer," J. Acoust. Soc. Am. **112**, 2026–2035.

Choy, Y. S., and Huang, L. (**2003**). "Drum silencer with shallow cavity filled with helium," J. Acoust. Soc. Am. **114**, 1477–1486.

Doak, P. E. (**1973**). "Excitation, transmission and radiation of sound from source distributions in hard-walled ducts of finite length. I. The effects of duct cross-section geometry and source distribution space-time pattern," J. Sound Vib. **31**, 1–72.

Ford, R. D., and McCormick, M. A. (**1969**). "Panel sound absorbers," J. Sound Vib. **10**, 411–423.

Frommhold, W., Fuchs, H. V., and Sheng, S. (**1994**). "Acoustic performance of membrane absorbers," J. Sound Vib. **170**, 621–636.

Fuchs, H. V. (**2001**). "From advanced acoustic research to novel silencing procedures and innovative sound treatments," Acta. Acust. Acust. **87**, 407–413.

Horoshenkov, K. V., and Sakagami, K. (**2001**). "A method to calculate the acoustic response of a thin, baffled, simply supported poroelastic plate," J. Acoust. Soc. Am. **110**, 904–917.

Huang, L., (**2002**). "Modal analysis of a drumlike silencer," J. Acoust. Soc. Am. **112**, 2014–2025.

Huang, L. (**2004**). "Parametric study of a drumlike silencer," J. Sound Vib. **269**, 467–488.

Huang, L. (**1999**). "A theoretical study of duct noise control by flexible panels," J. Acoust. Soc. Am. **106**, 1801–1809.

Huang, L., Choy, Y. S., So, R. M. C., and Chong, T. L. (**2000**). "Experimental studies on sound propagation in a flexible duct," J. Acoust. Soc. Am. **108**, 624–631.

Huang, L., Quinn, S. J., Ellis, P. D. M., and Ffowcs Williams, J. E. (**1995**). "Biomechanics of snoring," Endeavour **19**, 96–100.

Ingard, K. U. (**1994**). "Notes on the sound absorption technology," *Noise Control Foundation*, Poughkeepsie, N Y.

Maa, D.-Y. (**1975**). "Theory and design of microperforated panel sound absorbing constructions," Sci. Sin. **18**, 55–71.

Maa, D.-Y. (**1998**). "Potential of microperforated panel absorber," J. Acoust. Soc. Am. **104**, 2861–2866.

Mechel, F. P., and Vér, I. L. (**1992**). *Noise and Vibration Control Engineering: Principles and Applications*, edited by L. L. Beranek and I. L. Vér (Wiley, New York), Chap. 8.

Sakagami, K., Kiyama, M., Morimoto, M., and Takahashi, D. (**1996**). "Sound absorption of a cavity-backed membrane: A step towards design method for membrane-type absorber," Appl. Acoust. **49**, 237–247.